

Transport Processes at Single Droplets in Micellar Liquid/Liquid Systems

Niklas Paul and Matthias Kraume

Chair of Chemical and Process Engineering, Technische Universität Berlin, 13355 Berlin, Germany

Sebastian Schön and Regine von Klitzing

Stranski-Laboratorium für Physikalische und Theoretische Chemie, Institut für Chemie, Technische Universität Berlin, 10623 Berlin, Germany

DOI 10.1002/aic.14699

Published online December 19, 2014 in Wiley Online Library (wileyonlinelibrary.com)

In many industrial applications, the knowledge of the occurring transport processes in liquid/liquid systems is of great interest to design a multiphase reactor or an extraction column, for instance. All transport processes in liquid/liquid systems are governed by the interface. In some processes surfactants are needed. Surfactants change many interfacial properties which affect the transport processes. In this work, the influence of high surfactant concentrations (micellar systems) on transport processes is regarded. To understand, the occurring reduction of the drop rise velocity and of mass transfer rates experimental investigations of the occurring interfacial phenomena are carried out. Therefore, interfacial tension measurements as well as colloidal probe atomic force measurements of liquid/liquid systems were conducted. It was proved that for high nonionic surfactant concentrations a change of the phase behavior must be taken into consideration to describe transport processes in micellar liquid/liquid systems. © 2014 American Institute of Chemical Engineers AIChE J, 61: 1092–1104, 2015

Keywords: fluid dynamics, mass transfer, surfactants, micelles, liquid/liquid interfaces

Introduction

The understanding of transport processes in liquid/liquid systems is of special interest for many different industrial applications such as extraction processes or multiphase reactions. One of the most important multiphase reactions in the chemical industry is the hydroformylation of alkenes by the Ruhrchemie/Rhone-Poulenc process. In this process, water-soluble rhodium catalysts are used; hence the reactants have to be transported into the aqueous phase where the reaction takes place. For long chain alkenes, this process fails due to the low water solubility of these alkenes. Using surfactants, the water solubility of long chain alkenes is increased which results in higher reaction rates,^{1,2} but conversely, the presence of surfactant molecules will influence the transport processes, which again affects the yield and selectivity of multiphase reactions. The fundamental understanding of the influences exerted by surfactants on transport processes is of great interest to design a multiphase reactor or an extraction column, where a high surfactant concentration is expected. To lower the complexity of liquid/liquid systems only single droplets will be observed in this work. Therefore, complex swarm effects can be neglected.

While single droplets are rising in an aqueous-surfactant solution the surfactant molecules will adsorb at the interface

where a barrier layer is formed. This results in an additional mass transfer resistance.^{3–6} Furthermore, this adsorption layer of surfactant molecules leads to a change in the fluid dynamics: the liquid/liquid interface gets less mobile and the drag coefficient increases which results in a lower drop rise velocity. This change in the fluid dynamics affects the mass transfer rate as well. Droplets with mobile interfaces have inner circulations which improve mass transfer rates. These inner circulations are induced by shear stress, whereas particles with rigid interfaces do not have inner circulations. Therefore, the reduction of the inner circulations is also attributed to a decrease of mass transfer rates.^{7–10}

In most works cited in literature, a reduction of mass transfer with an increase of surfactant concentration was observed and this reduction was referred to the two phenomena aforementioned. But in most cases only low surfactant concentrations were observed where the surfactant concentration was lower than the critical micelle concentration (CMC). For multiphase reactions in micellar systems much higher surfactant concentrations have to be used to improve the reaction rate. In these cases, the two phenomena mentioned (change of the fluid dynamics and adsorption layer) are not enough.¹¹ For high nonionic surfactant concentrations, a change of phase behavior might need to be taken into account. Ternary systems consisting of water/oil/non-ionic surfactant change their phase conditions in dependence on their compositions (surfactant concentration) and temperature.¹² For isothermal conditions, many different types of structures can be found.¹³ Although, neither extraction

Correspondence concerning this article should be addressed to N. Paul at n.paul@mailbox.tu-berlin.de.

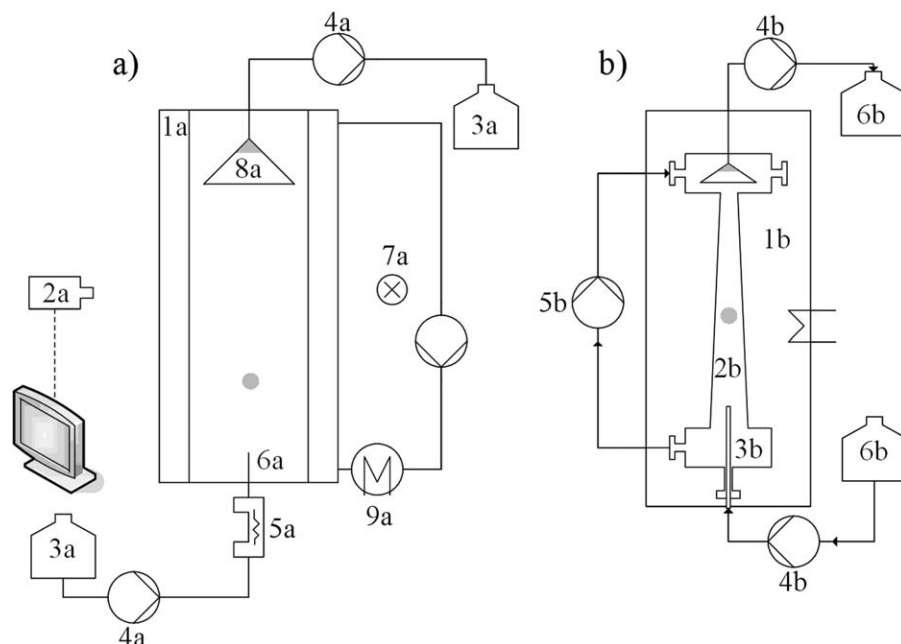


Figure 1. Experimental setups for the determination of the transport processes: (a) rising test cell: (1a) Glass column, (2a) high-speed camera, (3a) storage dispersed phase, (4a) Hamilton® PSD/2 modules, (5a) solenoid device, (6a) nozzle, (7a) illumination, (8a) glass funnel, (9a) thermostat; (b) counter flow cell: (1b) heating control, (2b) glass cone, (3b) nozzle, (4b) Hamilton® PSD/3 modules, (5b) gear pump, (6b) storage dispersed phase.

processes nor multiphase reactions should be designed at compositions where liquid crystals are formed, it is still possible that at the interface a composition is set up which leads to a formation of a microemulsion at the liquid/liquid interface or even a liquid-crystalline interface. Both would result in an additional mass transfer resistance.

The present study focuses on experimental investigations of transport processes in micellar systems. All transport processes in liquid/liquid systems are governed by the characteristics of the interface. Therefore, a detailed knowledge of the occurring interfacial phenomena exerted by surfactants is of great interest to understand the influences on the transport processes. In this work, the interfacial phenomena are observed by measurements of the interfacial tension for various surfactant concentrations. Furthermore, the rigidity of the liquid/liquid interface is measured by colloidal probe atomic force microscopy; with this technique a change of the phase behavior at the liquid/liquid interface can be determined. This information about the liquid/liquid interface in dependence of the surfactant concentration shall be applied to fluid dynamics and mass transfer measurements at single droplets.

Materials and Methods

Transport processes at single droplets (fluid dynamics and mass transfer) are determined in a special glass column and a counter flow cell. Another objective of this work is the analysis of interfacial phenomena exerted by surfactants. Interfacial tension is measured by the pendant drop method as well as the spinning drop method. Furthermore, the spring constant of the liquid/liquid interface is measured using colloidal probe atomic force microscopy.

Materials

For the experimental investigations a special test system is used, due to the highly sensitive measurements, all

components used are of high purity. The regarded testing system consisted of deionized water with a resistance of 18.3 MΩ cm, which is used as the continuous phase; 1-octanol (AppliChem, 99%) is applied as the dispersed phase. Avoiding additional transport processes both liquid phases were saturated with each other. Two different surfactants are utilized: the anionic surfactant sodium dodecyl sulfate (SDS; British Drug Houses Chemicals (BDH), 99%) and the non-ionic surfactant Triton X-100 (Merck, 99%, for analysis). The preparations of the parent surfactant solutions at 100 mmol/L are carried out by a Satorius balance with an uncertainty of 0.1 mg. Other surfactant concentrations were prepared by a serial dilution.

Experimental setup

The determination of the transport processes at single droplets was conducted in two different test cells. Both are shown in Figure 1. Figure 1a shows a rising test cell, which is used to determine the mass transfer as well as the fluid dynamics of single droplets.^{14,15} This test cell (rising test cell) consists of a glass column (1a) with a height of 1000 mm and a diameter of 75 mm. It is filled with water or aqueous-surfactant solution and surrounded by a jacket which is filled with glycerol, due to the similar refraction index to borosilicate glass. Every experiment is carried out at a temperature of 22 °C; to provide isotherm conditions a thermostat by LAUDA® is installed. A syringe pump (Hamilton® PSD/2 module) is used to generate a well defined drop volume of 1-octanol. The momentum-free drop release is realized by a solenoid device, also the droplets can be released at a specific volume, respectively, diameter. To provide a wide range of different droplet diameters the nozzles are changeable. In this work, only one borosilicate glass nozzle provided by Hilgenberg® was used. The installed glass nozzle had an outer diameter of 1.0 mm and an inner diameter of 0.42 mm. In a perpendicular position to the column a

Photonfocus® MV-752-160 high-speed camera (2a) is installed. The path of a droplet can be recorded by this camera. The analysis of the droplet's path is carried out with Image-Pro Plus® 5.1 by Media Cybernetics. As results the vertical and horizontal positions of the droplet are obtained. This information is used to calculate the instantaneous drop rise velocity. For the determination of the mass transfer a movable glass funnel is installed. At the neck of the glass funnel, a small amount of dispersed phase is kept, so the droplets can coalesce and be pumped out of the system by a second syringe pump. As the azo dye pyridine-2-azodimethyl-aniline (PADA) is used as the transferred component, the analysis of the dye concentration is carried out with a Specord 210 photometer by Jena Analytik®.

The counter flow test cell (Figure 1b) is also used for the determination of the mass transfer at single droplets, but with this experimental setup longer contact times can be realized. With the rising test cell (Figure 1a), the contact time is limited to the column's height. Whereas, the counter flow which is induced by the gear pump (Figure 1 [5b]) is able to realize a longer contact time. At some point in the cone (2b), the drop rise velocity equals the velocity of the counter flow and the droplet is able to be kept at one point. Therefore, the contact time can be chosen as long as the gear pump creates a counter flow. The analysis of the dye concentration in the droplets is conducted as in the rising test cell.

Interfacial tension measurements

The knowledge of the interfacial tension is of great importance in this work. On the one hand side it affects the drop formation. Additionally, it is possible to calculate the adsorption kinetics by applying the Gibbs–Duhem equation, respectively, the Langmuir–Szyskowski equation. Therefore, a DataPhysics OCA 20 is used as well as a Krüss SITE 04 to determine the interfacial tension in dependence of the surfactant concentration. Both methods had to be applied to measure the interfacial tension of the liquid/liquid system for various surfactant concentrations. The pendant drop method fails for interfacial tension values lower than 4 mN/m. Therefore, the spinning drop method has to be applied to measure low interfacial tension values as well.

Colloidal probe atomic force microscopy

Colloidal probe atomic force microscopy is applied for the determination of the mobility of the liquid/liquid interface. Basically, the experimental setup is described in Zeng and von Klitzing.¹⁶ A commercial atomic force microscope MFP3D (Asylum Research, distributed by Atomic Force Mannheim, Germany) is used. The experimental setup is shown in Figure 2 schematically. At the end of a tipless cantilever (CSC12, MikroMasch, Estonia), a silica sphere (Bangslabs) with a diameter of 6.7 μm is glued with epoxy glue. Before a measurement is started, the cantilever is cleaned with a plasma cleaner for 20 min. A polyether ether ketone (PEEK)-slide with eight equal holes (diameter: 1.6 mm) is used to produce eight droplets of the same size for statistical purpose, as the force measurements are highly sensitive to the droplet's diameter.¹⁶ After the holes are filled with 2 μL of water or aqueous-surfactant solutions, the droplets are covered with 2 mL 1-octanol.

After calibration of the system with the slope of the contact region on a hard surface the cantilever spring constant

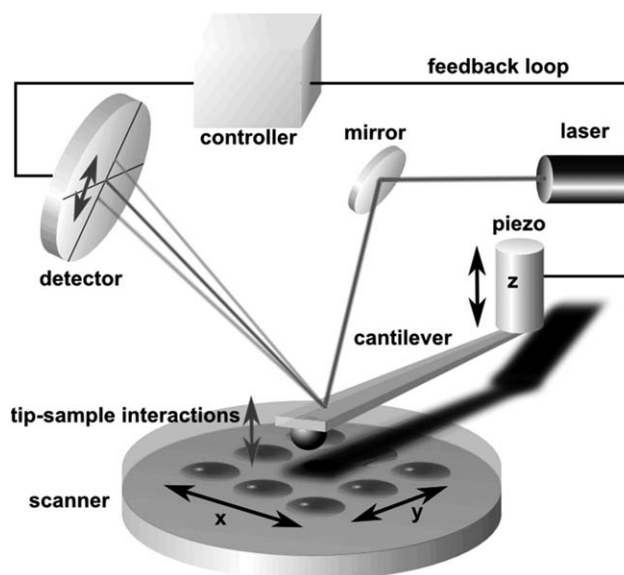


Figure 2. Schematic experimental setup: Colloidal Probe AFM.

was determined via the thermal noise method.¹⁷ The colloidal probe is brought into contact with the water-1-octanol interface and multiple force curves are measured. After conversion of the data into force-distance curves see Ducker et al.¹⁸ the linear slope can be used to calculate the spring constant of the interface. Thus, the obtained rigidity of the liquid/liquid interface has a huge impact on the fluid dynamics of single droplets.

Results

Interfacial tension

The CMC was determined for both surfactants used in this work. There are several methods to determine the CMC, in this work only the interfacial tension at the water/air interface was determined for various surfactant concentrations. For SDS, a value of 8.2 mmol/L was determined and for Triton X-100 a concentration of 0.2 mmol/L was measured for the CMC. Both values agree well with data from literature.^{19,20}

The dynamic interfacial tension at the water/1-octanol interface was determined for various surfactant concentrations. The surfactants used have exhibited different adsorption behavior. SDS showed very fast adsorption behavior; the value of the interfacial tension of the binary system water/1-octanol remained constant almost instantly. Figure 3 shows the dynamic interfacial tension for various SDS concentrations. SDS was soluted in the aqueous phase; hence the concentrations shown in Figure 3 represent the surfactant concentrations at the beginning of each measurement in the aqueous phase. While Figure 3a shows the results of the interfacial tension measurements by applying the spinning drop method Figure 3b gives the results carried out by the pendant drop method. For a clearer representation only the average values are shown. The deviations of the interfacial tension measurements obtained by both methods were <3%. The interfacial tension of the pure liquid/liquid system water-1-octanol was determined at 22 °C with a value of 8.1 mN/m. For both measurement techniques applied in this work, the value of the interfacial tension of the binary system water-1-

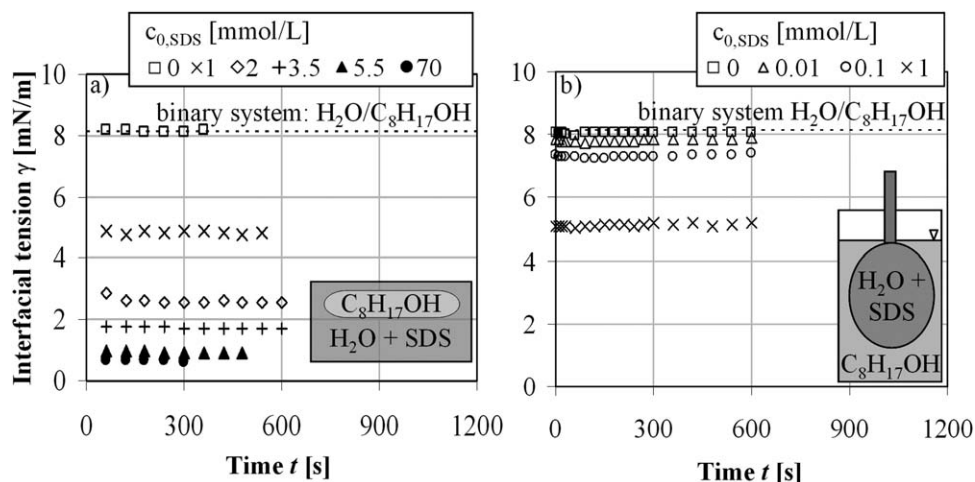


Figure 3. Dynamic interfacial tension of the binary system water-1-octanol for various concentrations of SDS: (3a) Measurements carried out by the spinning drop method; (3b) Measurements carried out by the pendant drop method.

octanol agrees well with the values given in the literature.²¹ For SDS concentrations lower than 0.01 mmol/L, there is almost no change in the interfacial tension observed. After exceeding SDS concentrations of 0.1 mmol/L, the interfacial tension is reduced until concentrations of 5.5 mmol/L are reached, then the interfacial tension remained constant. Both methods applied give the dynamic behavior of the interfacial time. SDS molecules are fast adsorbing molecules. Within, the first 60 s the equilibrium concentration at the interface is reached and the interfacial tension remains constant. Only small declines of the interfacial tension could be observed during the first seconds of the measurements.

Triton X-100 behaved differently than SDS. Figure 4 shows the unsteady interfacial tension (average values) for various Triton X-100 concentrations.

Figure 4a gives the dynamic interfacial tension for various Triton X-100 concentrations determined with the spinning drop method, whereas Figure 4b shows the results conducted by the pendant drop technique. The interfacial tension almost remains constant for Triton X-100 concentrations lower than the CMC (0.2 mmol/L). It was assumed that a decline of the interfacial tension occurs at lower concentrations than the CMC of the

air/water system as it was observed for the ionic surfactant SDS. Increasing the surfactant concentration beyond 1 mmol/L, the unsteady interfacial tension in Figure 4a progresses as expected with time. The adsorption kinetics of Triton X-100 is much slower than the kinetics of the ionic surfactant SDS (see Figure 3). The results of Figure 4a show, that after approximately 200 s the interfacial tension remains constant. Figure 4b gives a completely different dynamic behavior. Here, the interfacial tension decreases with time for the first seconds, but after certain point of time the interfacial tension increases again; hence a minimum occurs. This minimum gets more distinctive and appears earlier with higher Triton X-100 concentrations. The observed behavior is referred to transport processes. First, Triton X-100 molecules adsorb at the liquid/liquid interface, but get also transported into the 1-octanol phase;²³ hence, the dynamic interfacial tension is a function of the partition coefficient. The results given in Figure 4a were conducted by the spinning drop method. Here, 1-octanol droplets are generated in an aqueous-surfactant solution, whereas the result gained by applying the pendant drop method (Figure 4b) an aqueous-surfactant solution droplet is produced in the 1-octanol phase. The amount of surfactant molecules is the main difference

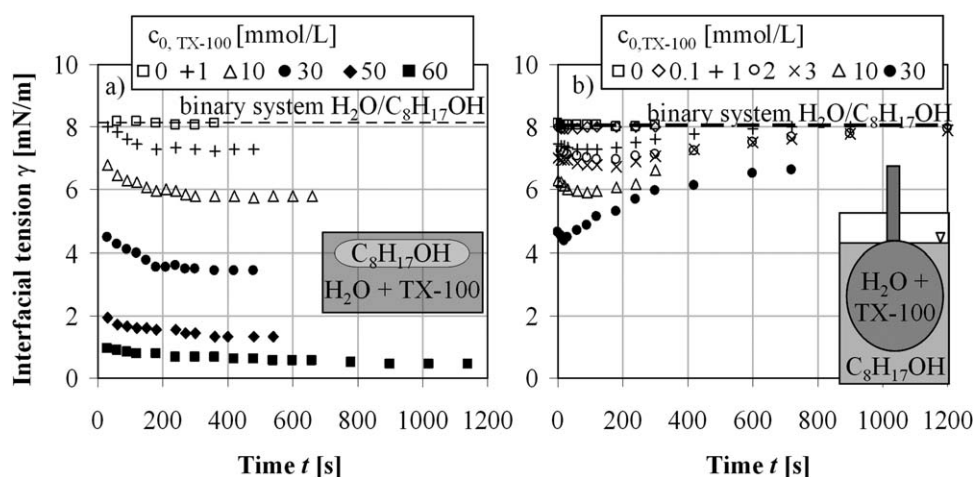


Figure 4. Dynamic interfacial tension of the binary system water-1-octanol for various Triton X-100 concentrations: (4a) Measurements carried out by the spinning drop method; (4b) Measurements carried out by the pendant drop method, data partly from.²²

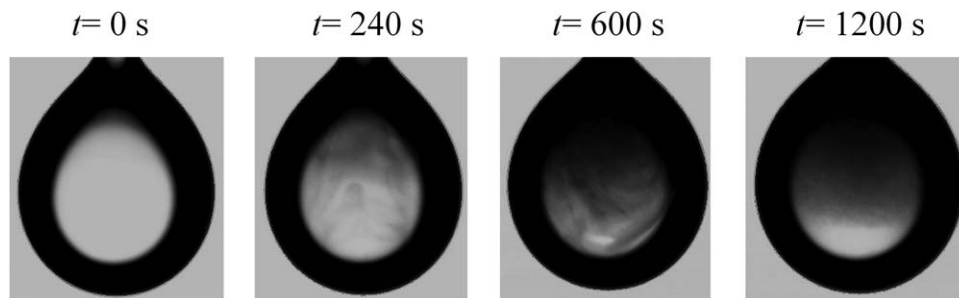


Figure 5. Water droplet with a Triton X-100 concentration of 2 mmol/L while measuring the interfacial tension by pendant drop method.

between both measurement techniques. Conducting the spinning drop method a small droplet is produced in an aqueous-surfactant solution; hence the amount of surfactant molecules seems to be infinite,²³ whereas the amount of molecules by applying the pendant drop method are limited.

Throughout the pendant drop measurements (Figure 4b) a strong movement of the droplet is observed. Furthermore, the droplets became blurry with time (Figure 5) although the phases have been saturated against each other. The four pictures shown in Figure 5 were taken at different point of times during one measurement. At the beginning of the measurement, the inside of the droplet was clear. After 180 s, a small haze appeared which started to increase as shown in Figure 5b. Furthermore, it moved chaotically inside the droplet as shown in Figure 5c. Additionally, a strong movement of the droplet was recognized in this period. After a certain time the internal flow of the cloudiness as well as the movement of the droplet settled down, the steady state was reached. This cloudiness can be referred to a change of the phase behavior. The ternary system water/1-octanol/Triton X-100 is able to change the phase behavior in many different ways.^{11,24} While the results given by Guo et al.²⁴ and by Paul et al.¹¹ referred to a whole system and give the equilibrium situation, the situation in this work is different. Here, an interfacial phenomenon is observed. The liquid/liquid interface can be considered as a pseudo phase with a high surfactant concentration and a certain amount of water and 1-octanol. Therefore, the formation of a liquid-crystalline layer or of a microemulsion is possible, which would explain the observed blurriness. In case of the interfacial tension measurements which were carried out in Figure 6 the droplet remained clear; no cloudiness was recognized during the determination of the interfacial tension. Therefore, the change of the clearness of the droplet is attributed to the formation of micelles which will form in the aqueous solution but could not be proven in the organic phase.²⁵

Figure 6 shows measurements of the interfacial tension by applying the pendant drop method, but in this case Triton X-100 was solved in 1-octanol. In these measurements, the dynamic progress of the interfacial tension decreased with time as expected, but the equilibrium surfactant concentration at the interface is reached very fast. The interfacial tension is hardly changing after the first seconds. Here, the amount of Triton X-100 molecules seem to be infinite like in the spinning drop measurements. Whereas, the results presented in Figure 4b show that the amount of surfactant molecules is limited and the transport has to be considered. The results of the interfacial tension measurements at the steady state agree well with the results gained by applying the spinning drop method (Figure 4a).

Figure 7 shows the influences of the surfactant concentration on the interfacial tension at steady state. To show the difference between the behavior of the interfacial tension at the liquid/air and at the liquid/liquid interface both dependencies are given in Figure 7. For both surfactants used in this work, a reduction of the interfacial tension with an increase of surfactant concentration is observed, but the adsorption behavior differs. Figure 7a gives the interfacial tension for various surfactant concentrations at the liquid/air interface. From this diagram, the values for the CMC can be derived ($c_{\text{SDS}} = 8.2$ mmol/L and $c_{\text{TX-100}} = 0.2$ mmol/L). Figure 7b shows the interfacial tension of the system water/1-octanol for various surfactant concentrations. Due to the occurring transport processes in presence of Triton X-100 only the results given in Figures 4a and 6 are shown in this diagram. In these cases, the surfactant was solved in the ambient phase; hence the amount of the surfactant can be considered as infinite and transport processes can be neglected at steady state.

Exceeding an SDS concentration of 1 mmol/L, the interfacial tension decreases approximately linearly due to the logarithmic scale of the diagram. After exceeding an SDS concentration of 5.5 mmol/L, the interfacial tension remains constant. Therefore, the CMC determined in the liquid/liquid system appears at lower concentrations than in the air/water system, which is assumed to be arising from the competition between the 1-octanol and surfactant molecules. For the

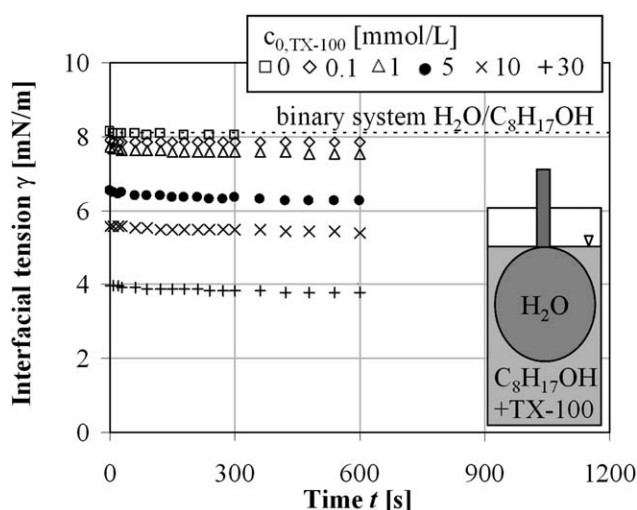


Figure 6. Dynamic interfacial tension of the binary system water-1-octanol for various Triton X-100 concentrations (Triton X-100 was solved in 1-octanol): Measurements carried out by the pendant drop method.

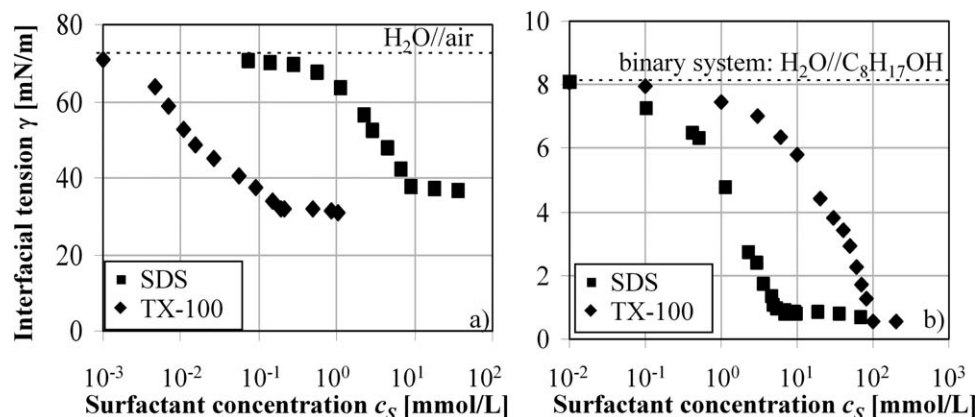


Figure 7. Interfacial tension depending on surfactant concentration at steady state at the liquid/air and at the liquid/liquid interface at 295 K.

nonionic surfactant Triton X-100, a completely different result was obtained; here, the reduction of the interfacial tension appears for higher surfactant concentrations than the CMC. Until the CMC (0.2 mmol/L) is not exceeded the interfacial tension did not change. For Triton X-100 concentrations higher than 40 mmol/L, a linear reduction of the interfacial tension is obtained. Exceeding Triton X-100 concentrations of 100 mmol/L, the interfacial tension remains constant. Therefore, the CMC in the liquid/liquid system was determined at a concentration of 100 mmol/L, which is three orders of magnitude higher than in the air/water system.

To explain the large CMC's shift, the composition of Triton X-100 has to be regarded. Although, Triton X-100 was used in the highest purity available, it still consists of a variety of molecules with different degrees of ethoxylation. With an increase of ethoxylation degree, the water solubility of the surfactant molecules, respectively, the hydrophilicity increases. Due to the different hydrophilicity in the range of molecules, the conditions at the liquid/air compared to the liquid/liquid interface differ. Figure 8 schematically gives the situations at the liquid/air and at the liquid/liquid interface. The schematic surfactant molecules with the big head group represent the molecules with the high degree of ethoxylation. These molecules are more hydrophilic than the molecules with the small head group; hence more energy is needed for those molecules to be transported to the interface, which makes them less interfacial active than the molecules with small ethoxylation degrees. Consequently, the concentration at the liquid/air interface of molecules with a high degree of ethoxylation is low. At the liquid/liquid interface the situation is different. Here, the hydrophobic

molecules are transported into the organic phase (see Figure 4b, also). Therefore, the concentration of the surfactant molecules with the smaller degree of ethoxylation at the liquid/liquid interface is lower than at the liquid/air interface. This effect was also observed in the work of Daniel and Berg.²⁶ Here, Tergitols with different degrees of ethoxylation were observed and it was shown that CMC values shift to lower values with decreasing degree of ethoxylation.

The results of the interfacial tension measurements are used to calculate the coverage of the interface by surfactant molecules. As described above with an increase of the interfacial coverage a reduction of the transport processes is expected. Therefore, the knowledge of the interfacial coverage is useful tool describing the assumed effects on the transport processes.

Interfacial coverage

The relationship between the interfacial tension and the interfacial coverage is given by the Gibbs–Duhem equation which is valid at constant temperature and constant pressure²⁷

$$\sigma d\gamma + \sum_i n_i(\sigma) d\mu_i = 0. \quad (1)$$

The chemical potential μ can be substituted by the concentration. Therefore, the equation can be written as

$$\Gamma = - \frac{1}{nRT} \frac{d\gamma}{d \ln c}, \quad (2)$$

where Γ is the concentration of surfactants at the interface. Applying this equation to the results of Figure 7b, it is

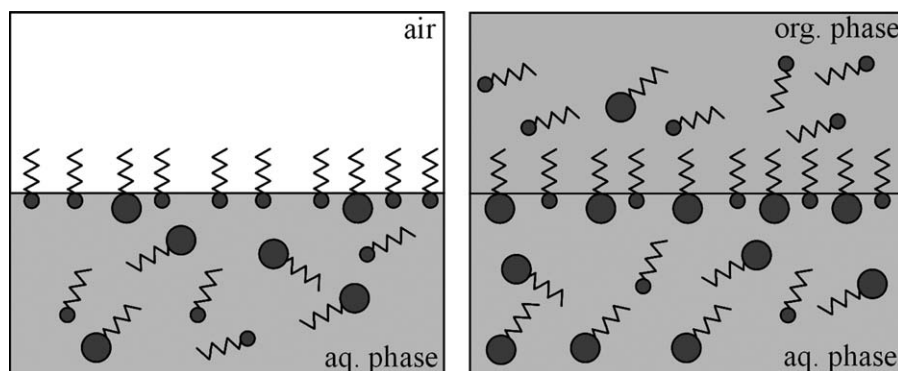


Figure 8. Situations at the liquid/liquid interface and the gas/liquid interface (schematically).

Table 1. Langmuir Constants in the Liquid/Liquid System Water/1-Octanol for the Used Surfactants

	SDS	Triton X-100
Γ_{\max} [$\mu\text{mol}/\text{m}^2$]	0.5	17.5
b [mol/m^3]	0.0003	0.91

possible to calculate the maximal surfactant concentration by the determination of the slope $d\gamma/d\ln c$. If, the slope is constant with the start of the decline of the interfacial tension; the surfactant concentration at the interface is approximately constant in this region.²⁸ That means that the coverage of the interface is almost completed at a concentration of 40 mmol/L Triton X-100 (see Figure 7b). Strictly speaking Eq. 2 is valid for pure surfactants only. As already mentioned Triton X-100 was used in analytical quality but nevertheless consists of a distribution of molecules with different ethoxylation degrees. Therefore, conclusions based on the application of this equation on the results connected to TritonX100 have to be handled with care.

Another possibility for calculating the maximal interfacial surfactant concentration is applying the Langmuir–Syskowski isotherm²⁹

$$\pi^\gamma = -nRT\Gamma_{\max} \ln\left(\frac{c}{b} + 1\right), \quad (3)$$

where π^γ ($\pi^\gamma = \gamma_0 - \gamma_s$) is the interfacial pressure, Γ_{\max} is the maximal interfacial concentration of the surfactant (complete coverage) and b is the Langmuir constant which shows the relationship between the desorption rate and the adsorption rate of the surfactant molecules at the interface. By applying Eqs. 2 and 3 to the experimental data gained from the interfacial tension measurements, the results for the Langmuir constants (Γ_{\max}) are the same. The results are given in Table 1. The adsorption behavior of both surfactants is very different, as already assumed from the results of the interfacial tension. Both surfactants have completely different ratios of the desorption rate to the adsorption rate. For SDS, a very small value of 0.0003 mol/m³ was determined. This shows the fast adsorption at the liquid/liquid interface, which was observed while determining the dynamic interfacial tension. Here, the interfacial tension was immediately constant; whereas a constant value for the interfacial tension of the nonionic surfactant Triton X-100 was observed after a much longer time. The high value of b for Triton X-100 with 0.91 mol/m³ being close to unity implies that the desorption rate is almost as high as the adsorption rate.

Comparing the results given in Table 1 with the values which can be determined for the air/liquid system (Figure 7) show unexpected results for the nonionic surfactant Triton X-100. The interfacial concentration of Triton X-100 increased by a factor of 5.5 compared to the measurements at the air/liquid interface ($\Gamma_{\max, l, l} = 17.5/\Gamma_{\max, g, l} = 3.15$). At the liquid/liquid interface a lower interfacial concentration is assumed due a concurrence situation between Triton X-100 and the amphiphilic 1-octanol molecules. The increase of the interfacial concentration was referred to the additional change in the phase behavior as mentioned above (see Figure 5). For SDS, the interfacial concentration was decreased by a factor of 5 compared to the measurements at the air/liquid interface ($\Gamma_{\max, l, l} = 0.5/\Gamma_{\max, g, l} = 2.5$). This is referred to 1-octanol molecules which lower the number of adsorption places for Triton X-100.

The values given in Table 1 can be used to calculate the interfacial concentration of surfactant molecules for various surfactant concentrations in the bulk phase by applying the Langmuir isotherm

$$\Gamma = \frac{\Gamma_{\max} c}{c + b} \text{ and } \Phi = \frac{\Gamma}{\Gamma_{\max}}, \quad (4)$$

where Φ is the interfacial coverage of surfactant molecules. Figure 9 shows the calculated interfacial coverage in dependence of the surfactant concentration by applying Eq. 4 and using the results of Table 1.

With an increase of the surfactant concentration in the bulk phase, the surfactant coverage of the liquid/liquid interface rises until the saturation concentration is reached. This is observed for both surfactants. For SDS, the complete coverage is reached a bit below the CMC, as it is assumed.²⁸ Whereas, Triton X-100 shows a different behavior; here, the complete coverage is neither reached at the CMC concentration (0.2 mmol/L) nor at the “CMC” concentration in the liquid/liquid system (100 mmol/L). As aforementioned, the validity of Eq. 2 has to be taken into consideration. But it also could imply that something else is happening at the interface than just adsorption of surfactants at the liquid/liquid interface, which makes the standard procedure of calculating the interfacial coverage fail. Triton X-100 molecules adsorb, which will lead to a high local surfactant concentration there. Furthermore, water molecules will be attracted by the polar head group of the surfactants; hence a high water and surfactant concentration is set up which leads to the formation of high viscous multiphase conditions at the interface or even the formation of liquid crystals at the interface. This would result in a rigid liquid/liquid interface.

Colloidal probe atomic force microscopy

To determine the rigidity of the liquid/liquid interface colloidal probe atomic force microscopy was applied as described above. Figure 10 shows the results of the liquid/liquid interface's spring constant in dependence of the surfactant concentration. The spring constant is normalized to the value of the pure liquid/liquid system. To be sure that the system is in the equilibrium; all measurements were started after waiting for 20 min. For a better understanding of the gained results, the interfacial tension is plotted in this

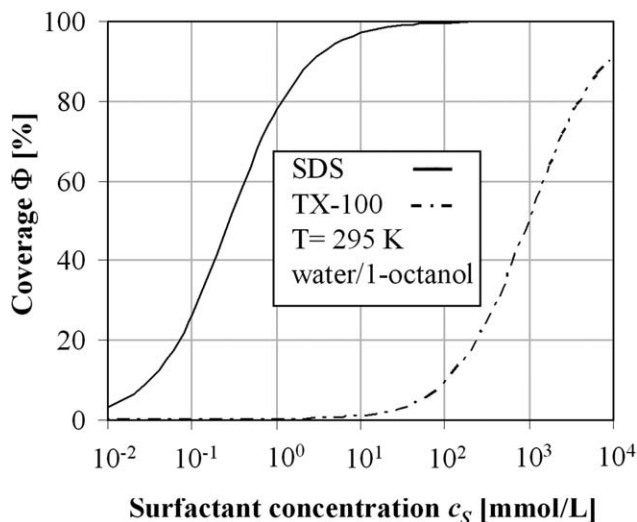


Figure 9. Interfacial coverage in dependence of the surfactant concentration.

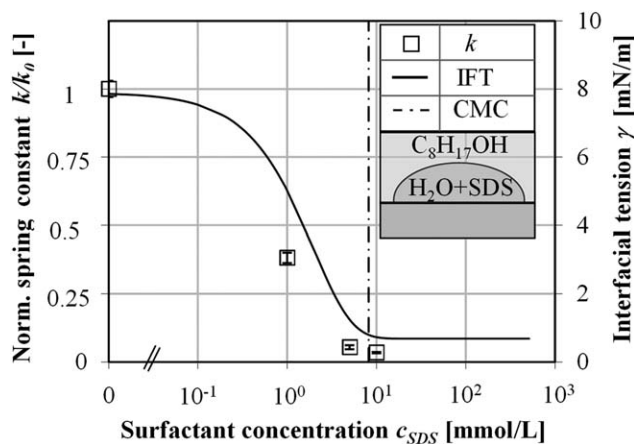


Figure 10. Spring constant of the liquid/liquid interface (water-1-octanol) in dependence of the surfactant concentration (SDS in aqueous phase).

diagram as well. With increasing the surfactant concentration the interfacial tension of the liquid/liquid system reduces; hence the spring constant of the liquid/liquid interface decreases. This result was expected. By reducing the interfacial tension, the interfacial energy decreases and less force is needed to deform the liquid/liquid interface. The interfacial tension is directly proportional to the spring constant of a liquid/liquid interface. Attard and Miklavcic describe the spring constant with the following equation³⁰

$$k = \frac{-4\pi\gamma}{\frac{\cos \theta}{2 + \cos \theta} + \ln \left[\frac{R_d}{2\kappa R_d^2} \frac{(1 + \cos \theta)^2}{\sin^2 \theta} \right]} \quad (5)$$

where γ is the interfacial tension, θ is the contact angle, R_d is the radius of the droplet, and κ is the interaction decay. From this equation, the linear relationship between the interfacial tension and the spring constant can be derived. This dependency is observed in Figure 10. The progress of the interfacial tension and the spring constant with increasing SDS concentrations is almost parallel.

The same colloidal probe measurements at the water/1-octanol interface have been carried out with Triton X-100. Figure 11 shows the normalized spring constant for various Triton X-100 concentrations. Also, the interfacial tension is plotted in this diagram. For small Triton X-100 concentrations, the spring constant of the liquid/liquid interface remains constant. For higher Triton X-100 concentrations than 10 mmol/L, the spring constant decreases linearly (due to the logarithmic scale of the diagram) and shows a direct proportionality to the progress of the interfacial tension. This behavior was expected and is predicted by Eq. 5. Figure 12 shows the results of similar measurements, except Triton X-100 was solved in the aqueous phase and not in the organic phase as in the results given in Figure 11. Here, the situation is different a direct proportionality between the interfacial tension and the spring constant of the liquid/liquid interface is only given for Triton X-100 concentrations smaller than 1 mmol/L. For higher Triton X-100 concentrations, the spring constant decreases linearly until concentrations of 10 mmol/L are reached, beyond this concentration the spring constant remains constant. This behavior is not expected. With decreasing values of the interfacial tension a reduction of the liquid/liquid spring constant is expected. The constant values of the spring constant are evidence for

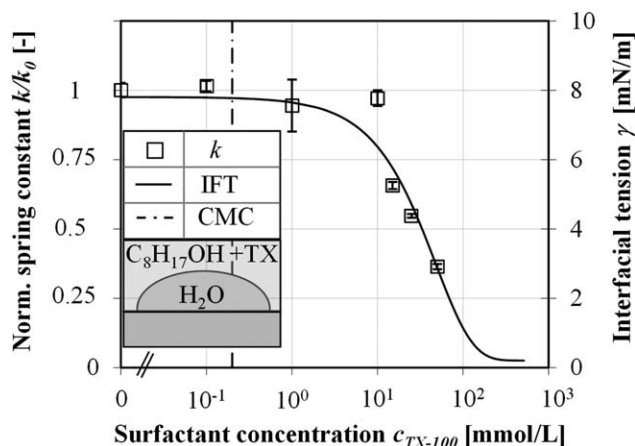


Figure 11. Spring constant of the liquid/liquid interface (water-1-octanol) in dependence of the surfactant concentration (Triton X-100 in organic phase).

the formation of new interface at the droplet. This assumption is reinforced by the occurring cloudiness at the liquid/liquid interface, which was observed through the microscope camera for Triton X-100 concentrations higher than 1 mmol/L. This phenomenon was only observed when Triton X-100 was solved in the aqueous phase. Throughout the other measurements (Figures 10 and 11), the liquid/liquid interface remained clear.

While in the aqueous phase micelles occur at Triton X-100 concentrations beyond 0.2 mmol/L micelles were not found in pure organic solvents.²⁵ Therefore, the presence of micelles is the major difference between the results given in Figures 11 and 12. This situation is given in Figure 13 schematically. For Triton X-100 concentration higher than the CMC micelles form and are able to solubilize the organic solvent. In the area near by the liquid/liquid interface, the surfactant concentration is high. Additionally, a certain amount of organic solvent has to be considered at the liquid/liquid interface; hence compositions might occur which form a high viscous micro-emulsion-phase or even a liquid-crystalline phase, if the micelles have a certain long range order at the interface. This

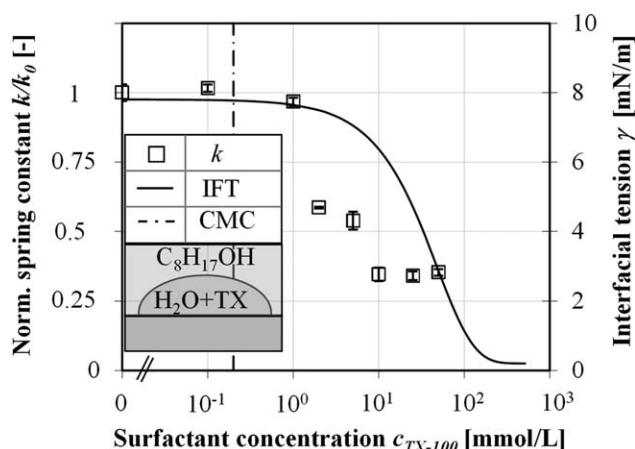


Figure 12. Spring constant of the liquid/liquid interface (water-1-octanol) in dependence of the surfactant concentration (Triton X-100 in aqueous phase).

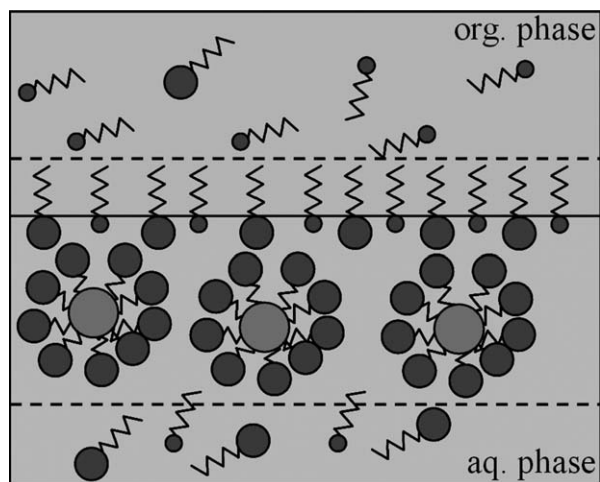


Figure 13. The formation of a microemulsion at the interface (schematically).

formation of the new liquid/liquid interface is able to influence the occurring transport processes.

Furthermore, the increase in rigidity or stiffness of the liquid/liquid interface is obtained by regarding the progress of the deflection throughout a measurement (Figure 14). At low surfactant concentrations (<10 mmol/L), the colloidal probe always stuck to the interface. Figure 14a schematically shows the deflection in dependence of the distance to the interface. In this case, the colloidal probe was always in contact with the interface. For concentrations higher than 10 mmol/L this was not observed; here, the colloidal probe released from the interface while the pressure on the interface was loosened. Figure 14b schematically shows that while the colloidal probe is drawn back from the surface the deflection jumps at one point to its initial position. This jump of the deflection can be explained by the decrease of the interface's mobility; when the colloidal probe moves away from the liquid/liquid interface, the interface is to inflexible to stay in contact. Another explanation for the change in the progress of the deflection signal could be that the hydrophilicity of the liquid/liquid interface changed, due to the increase of the interfacial coverage with surfactant molecules. The hydrophobic tails of Triton X-100 molecules will reach out of the liquid/liquid interface; hence the

hydrophilicity at the interface is reduced with an increase of surfactant concentration. Therefore, the hydrophilic silica sphere which is attached to the cantilever did not stay in contact with the liquid/liquid interface.

Fluid dynamics of single droplets

The fluid dynamics of single droplets is observed by applying the rising test cell (Figure 1a). With a high-speed camera the droplet's path is recorded from droplet's release until it coalesced in the funnel. The analysis of the droplet's path was carried out with Image-Pro Plus® 5.1 by Media Cybernetics. The instantaneous drop rise velocity was the result of this analysis.

By the characterization of the fluid dynamics of single droplets, it is possible to probe the coverage of liquid/liquid interfaces with surfactant molecules, as the fluid dynamics reflects the rigidity of liquid/liquid interfaces. For a high interfacial coverage, the interface of a fluid particle becomes less mobile. Hence, the drag coefficient increases and the drop rise velocity decreases. Figure 15 shows the instantaneous drop rise velocity for 2.5 mm droplets. For a clear representation, only one representative track out of at least 15 recorded tracks for each surfactant concentration is shown. The reproducibility of these measurements was high; the uncertainty of each measurement was <2.5%.

The coverage of the droplet's interface increases with increasing surfactant concentration in the continuous phase (see Figure 9), leading to decreasing drop rise velocities, due to the lower flexibility of the interface as it is proofed by the colloidal probe AFM measurements. In the surfactant-free case, the droplet rises like a fluid particle with a free moveable interface. Due the high viscosity ratio between 1-octanol droplet water ($\eta^* = 10$) the correlation by Feng and Michaelides³¹ can be applied to calculate the drop rise velocity. This correlation is valid for high viscosity ratios ($2 < \eta^* < \infty$) and Reynolds numbers in the range of 5 and 1000. For 2.5 mm droplets that rise at a velocity of approximately 95 mm/s a corresponding Reynolds number of 240 was calculated; hence the correlation is valid. The experimental results agree well with the calculated results by solving the correlation of Feng and Michaelides,³¹ respectively, the differential equation system^{32,33}

$$\frac{dv_p}{dt} = \frac{\rho_p - \rho_f}{\rho_p + \alpha\rho_f} g - \zeta \frac{\rho_f}{\rho_p + \alpha\rho_f} \frac{3}{4d_p} v_p^2, \quad (6)$$

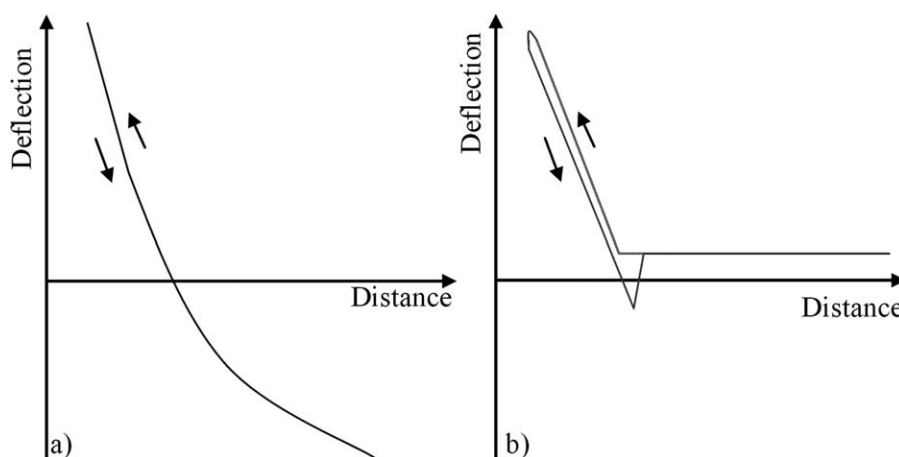


Figure 14. Deflection in dependence on of the distance (schematically): (a) for a mobile interface the probe is always in contact with the interface (b) for a rigid interface the probe is released from interface.

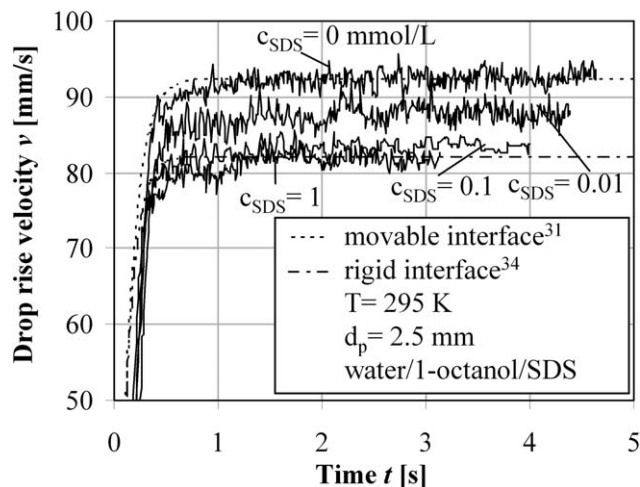


Figure 15. Instantaneous drop rise velocity for 2.5 mm 1-octanol droplets in different aqueous-surfactant (SDS) solutions, data partly from.²²

where α is the critical mass, v_p is the instantaneous drop rise velocity, and ζ is the drag coefficient which can be calculated by a correlation for a constant movement of a spherical droplet³¹

$$\zeta(Re, \eta^*) = \frac{4}{\eta^* + 2} \zeta(Re, 2) + \frac{\eta^* - 2}{\eta^* + 2} \zeta(Re, \infty). \quad (7)$$

A reduction of the drop rise velocity was observed at an SDS concentration of 0.01 mmol/L. At lower concentrations, the drop rise velocity is hardly affected by surfactants. Exceeding a surfactant concentration of 1 mmol/L, the droplet behaves like a particle with a rigid interface, which is the other borderline case. The calculation can also be carried out by solving the differential equation system represented by Eq. 6 and using the correlation³⁴

$$\zeta = \frac{1}{3} \left(\sqrt{\frac{72}{Re}} + 1 \right)^2. \quad (8)$$

Additionally, it is possible with these measurements of the unsteady drop rise velocity to characterize the adsorption kinetics of surfactants at liquid/liquid interfaces. For slow adsorbing surfactants, the coverage of the liquid/liquid interface increases with time; hence a reduction of velocity is recognized after the acceleration of the droplet, a maximum velocity value is the result. This is not observed in Figure 15. Here, the droplets accelerate in the first second and afterward the drop rise velocity remains constant. This result is confirmed by the results of the interfacial tension measurements. In Table 1, the Langmuir constants are given. For b a small value was determined, which means that the adsorption rate is much faster than the desorption rate. Therefore, the adsorption of SDS molecules is completed within in the first second. Otherwise, a decrease of drop rise velocity with time should be observed.

Wegener and Paschedag³⁵ observed in the system water-toluene-SDS a maximum in drop rise velocity for small SDS concentrations. As shown above a maximum was not observed in this work. The adsorption behavior of SDS is different in both liquid/liquid systems. Adsorption at the liquid/liquid interface of SDS is even more favored in water-toluene than in water-1-octanol. A value for b of $7 \cdot 10^{-6}$ mol/m³ for

water-toluene is found in the literature.³⁶ Whereas, the value given in Table 1 is higher; hence the adsorption of SDS is more favored in the system water-toluene. Furthermore, the maximal interfacial concentration Γ_{\max} is approximately two times higher in the system water-toluene³⁷ than in the system water-1-octanol. Therefore, there are much more adsorption places for surfactant molecules at the water-toluene interface, which can be occupied during the rise of the droplet; hence the drop rise velocity decreases with time.³⁵ Additionally, the drop rise velocity of a particle with a rigid interface is reached at lower SDS concentrations for the system water-toluene than for water-1-octanol. For SDS concentrations of 10^{-3} mmol/L, toluene droplets behave like rigid particles. That is referred to the faster adsorption of SDS and to the lower equilibrium concentration at the interface in the toluene-water system than in the water-1-octanol system; here, SDS concentrations of 0.1 mmol/L reduce the drop rise velocity to the velocity of a droplet with a rigid sphere.

In Figure 16, the impact on drop rise velocity of a non-ionic surfactant (Triton X-100) for 2.5 mm droplets is obtained in the system water-1-octanol. Compared to the results in Figure 15, the behavior is a bit different. After exceeding a surfactant concentration of 0.01 mmol/L the drop rise velocity is reduced. For gas bubbles less Triton X-100 is needed to immobilize the interface.³⁶ In the work of Takagi and Matsumoto,³⁶ the gas bubbles behaved like rigid spheres for Triton X-100 concentrations of $7 \cdot 10^{-4}$ mmol/L. This is in the same order of magnitude as in the work of Wegener and Paschedag.³⁵ As aforementioned, the differences of the surfactant impact on the drop rise velocity between the regarded test systems arise from the variability of the adsorption behavior in the systems. In the work of Lee,⁶ falling tetrachloromethane droplets in an ambient aqueous-surfactant solution were observed, the adsorption behavior of this system is more comparable to water/octanol. Therefore, the results gained in this work (water/octanol) are more comparable to the work of Lee.⁶

For Triton X-100 concentrations of 0.1 mmol/L, a maximum is observed in drop rise velocity. That is referred to the slow adsorption kinetics of Triton X-100 molecules. The interfacial tension measurements already showed that

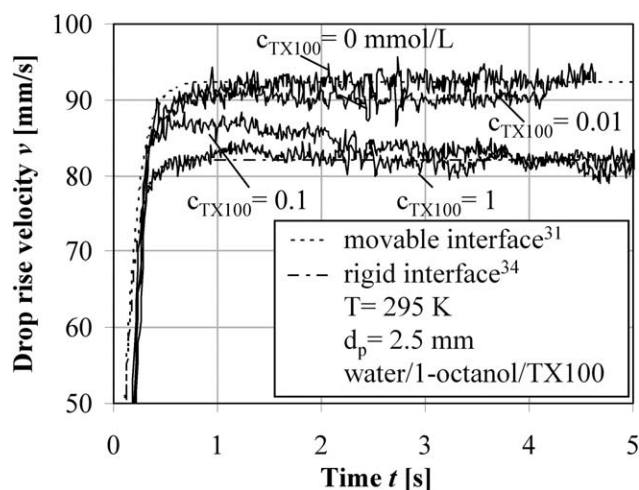


Figure 16. Instantaneous drop rise velocity for 2.5 mm 1-octanol droplets in different aqueous-surfactant (Triton X-100) solutions, data partly from.²²

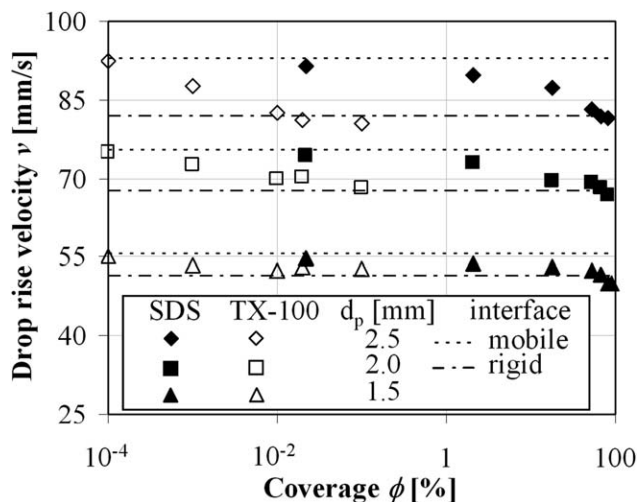


Figure 17. Terminal drop rise velocity in dependency of the interfacial coverage with surfactant for different droplet diameters and the limits free moveable interface, respectively, rigid interface, data partly from,²²

reaching the equilibrium interfacial surfactant concentration takes a long time. Hence, the equilibrium concentration is not reached after 1 s as it is observed in Figure 15. The saturation of the interface continues while the droplet is rising. Therefore, the drop rise velocity decreases slowly with time until it approaches the drop rise velocity of a particle with a rigid interface. For higher surfactants concentrations, the velocity maximum is less distinctive; hence higher interfacial concentrations are set up faster, so the drop rise velocity of a rigid particle is reached earlier. These results agree with the results of Kurimoto et al.³⁷ Where a concentration of 1 mmol/L was used to observe completely covered droplets. Marangoni effects which might occur due to the adsorption and desorption of the surfactant molecules at the interface cause gradients of the interfacial tension and exert oscillations of the droplets.¹⁵ This was not observed in this test system. Furthermore, a reacceleration of the droplet was not observed as observed

in the work of Wegener et al.^{14,15} Therefore, the reduction of the drop rise velocity is referred to the adsorption of surfactant molecules.

For Triton X-100 (in water/1-octanol) these results are unexpected; due to the interfacial tension measurements, respectively, to the calculation of the interfacial coverage. For the Triton X-100 concentrations regarded in Figure 16 actually no adsorption of surfactant molecules is assumed (Figure 9). But the fluid dynamics of the single droplets imply that the coverage is completed, because of the reduction of the drop rise velocity. To compare both results of the interfacial measurements and the fluid dynamics; the terminal drop rise velocity is plotted depending on the coverage.

Figure 17 shows that the assumptions in the literature for SDS are confirmed. For a high interfacial coverage with surfactant molecules the drop rise velocity decreases to a velocity value of a particle with a rigid interface. Whereas, for Triton X-100 the results of the interfacial tension measurements and the fluid dynamics do not match at all. For very low interfacial coverage of almost 0.1% the fluid droplet behaves like a particle with a rigid interface. Therefore, something other than adsorption of surfactants at the interface has to be taken into account for the reduction of the drop rise velocity. Also, the ability of surfactants to change the phase behavior of a liquid/liquid system must be considered. The formation of complex and high viscous multiphase systems at the liquid/liquid interface in presence of Triton X-100 was testified by colloidal atomic force measurements. Therefore, the reduction of drop rise velocity is explained by the formation a multiphase system at the liquid/liquid interface, which was determined during the colloidal probe measurements and causes a less mobile interface; hence the drag coefficient increases and the drop rise velocity decreases. These results can be used to predict the mass transfer at single droplets. For Triton X-100 concentrations higher than 1 mmol/L, a complete coverage is predicted from the fluid dynamic point of view. Therefore, a further reduction of the mass transfer is not expected. But due to other interfacial phenomena than adsorption an additional mass transfer resistance occurs.¹¹ This was proven by the AFM-measurements in this

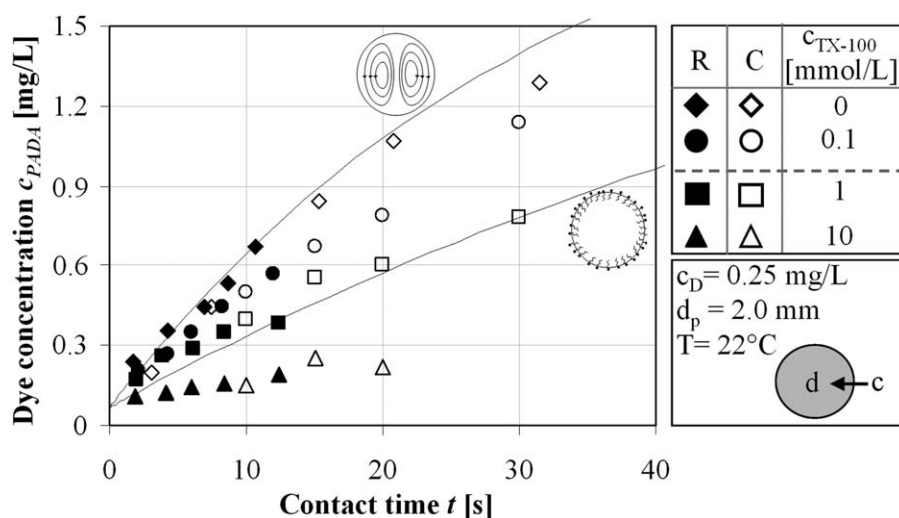


Figure 18. Unsteady mass transfer for various surfactant concentrations at single droplets with a diameter of 2 mm. Calculated progresses of the limiting cases: Freely movable interface³⁸ and droplet with a rigid interface.^{38,39}

work or with oscillating drop measurements (increase of the interfacial rheology) in.¹¹

Mass transfer at single droplets

Figure 18 shows the unsteady mass transfer at single droplets for various Triton X-100 concentrations. Triton X-100 was soluted in the continuous (aqueous) phase. The transport direction was chosen from the continuous phase into the dispersed phase. In presence of high SDS concentrations, the mass transfer could not be determined, due to the adsorption layer of SDS molecules at the liquid/liquid interface the droplets did not coalesce; hence it was impossible to determine the correct contact time. Besides, the experimental results calculated values are given for the two limiting cases: droplet with a freely movable interface³⁸ and a droplet with rigid interface.³⁹ The experimental results gained with both test cells (R = rising test cell and C= counter flow test cell) are given in this diagram. Both techniques agree well with each other. Furthermore, the experimental results for the pure system agree well with calculated dynamic progress of the dye concentration. For high surfactant concentrations, it was assumed that the mass transfer resistance becomes constant, due to the coverage of the liquid/liquid interface with Triton X-100 molecules. But at 10 mmol/L the mass transfer resistance increases and the mass transfer rate decreases to a much lower rate than the limiting case of a droplet with a rigid interface. This can be explained by the colloidal probe atomic force microscopy measurements shown above. With this measurement technique, it was shown that at concentrations of approximately 10 mmol/L Triton X-100 the formation of microemulsion layer or even a liquid-crystalline layer at the interface is possible. Therefore, the mass transfer resistance increases and does not remain constant at concentrations higher than the CMC; hence the change in phase behavior must be taken into account otherwise the transport processes are over predicted.

Conclusions

Transport processes of single droplets in liquid/liquid systems have been observed in this work. A reduction of the drop rise velocity with increasing surfactant concentration was obtained as it was expected. For the ionic surfactant SDS, the phenomena given in the literature can be used to explain the reduction of drop rise velocity. By determining the adsorption behavior of SDS at the liquid/liquid interface from the interfacial tension measurements, it was obtained that with an interfacial coverage of 60% the 1-octanol droplet behaves like a particle with a rigid interface. For Triton X-100, this explanation can not be used. The results of the interfacial tension measurements and the fluid dynamics are contrary to each other. Coverage of <1% was enough so that 1-octanol droplets rose like particles with rigid interfaces. Colloidal atomic force measurements were applied to probe the formation of high viscous multiphase systems at the liquid/liquid interface which decreased the mobility of droplet's interface and increased the drag coefficient, which ended up in a reduction of the drop rise velocity. Therefore, in presence of Triton X-100 the phase behavior of the liquid/liquid system has to be observed. These results are also reflected in the determination of the mass transfer. The mass transfer rates were decreased dramatically for high surfactant concentrations. This behavior cannot be explained with the

two phenomena given in the literature this underlines the necessity to regard the phase behavior of micellar liquid/liq-uid systems for transport processes.

Furthermore, it was testified that surfactants do not affect the fluid dynamics of single droplets in the same way comparing different liquid/liquid systems. The adsorption behavior of the corresponding liquid/liquid system has also to be regarded.

Acknowledgments

This work is part of the Collaborative Research Centre "Integrated Chemical Processes in Liquid Multiphase Systems" coordinated by the Technische Universität Berlin. Financial support by the Deutsche Forschungsgemeinschaft (DFG) is gratefully acknowledged (TRR 63 sub-projects A6 and B8, KL1165/10-3).

Notation

Symbols

c = concentration, mol/L
 d = diameter, mm
ID = inner diameter, mm
 k = spring constant, mN/m
 n = number of ions
 N = nozzle
OD = outer diameter, mm
 R = gas constant, J/(mol K)
 t = time, s
 T = temperature, °C
 v = drop rise velocity, mm/s
 R = drop radius, m

Greek letters

γ = interfacial tension, mN/m
 Γ = interfacial concentration, mol/m²
 μ = chemical potential, J/mol
 Φ = coverage at the interface, %
 σ = Area, m²
 ζ = drag coefficient
 κ = interaction deca, nm
 θ = contact angle, °

Subscripts

0 = no surfactant
Cs = surfactant concentration
D = droplet
Max = Maximal
P = Particle
S = surfactant

Dimensionsless numbers

Re = Reynolds number

Shortcuts

AFM = atomic force microscopy
CMC = critical micelle concentration
SDS = sodium dodecyl sulfate
TX-100 = Triton X-100

Literature Cited

- Dwars T, Paetzold E, Oehme G. Reaktionen in mizellaren Systemen (in German). *Angew Chem*. 2005;117:7338–7364.
- Hamerla T, Rost A, Kasaka Y, Schomäcker R. Hydroformylation of 1-dodecene with water-soluble rhodium catalysts with bidentate ligands in multiphase systems. *ChemCatChem*. 2013;7:1854–1862.
- West FB, Herrman AJ, Chong AT, Thomas LEK. Addition agents and interfacial barriers in liquid/liquid extraction. *Ind Eng Chem*. 1952;44:625–631.
- Lindland KP, Terjesen SG. The effect of a surface-active agent on mass transfer in falling drop. *Chem Eng Sci*. 1956;5:1–12

5. Chen LH, Lee YL. Adsorption behavior of surfactants and mass transfer in single-drop extraction. *AIChE J.* 2000;46:160–168.
6. Lee YL. Surfactants on mass transfer during drop-formation and drop falling stage. *AIChE J.* 2003;49:1859–1869.
7. Gibbons JH, Houghton G, Coull J. Effect of a surface active agent on the velocity of rise of benzene drops in water. *AIChE J.* 1962;8:274–276.
8. Wegener M, Paul N, Kraume M. Fluid dynamics and mass transfer at single droplets. *Int J Heat Mass Transfer.* 2014;75:475–495.
9. Griffith RM. The effect of surfactants on the terminal velocity of drops and bubbles. *Chem Eng Sci.* 1962;17:1057–1070.
10. Beitel A, Heideger WJ. 1971. Surfactant effects on mass transfer from drops subject to interfacial instability. *Chem Eng Sci.* 1971;26:711–717.
11. Paul N, Schrader P, Enders S, Kraume M. Effects of phase behaviour on mass transfer in micellar liquid/liquid systems. *Chem Eng Sci.* 2014;115:148–156.
12. Kahlweit M, Strey R. Phasenverhalten ternärer Systeme des Typs H₂O-Öl-nichtionisches Amphiphil (in German). *Angew Chem.* 1985;97:655–669.
13. Larson RG. Self-assembly of surfactant liquid crystalline phases by Monte Carlo simulation. *J Chem Phys.* 1989;91:2479–2488.
14. Wegener M, Grünig J, Stüber J, Paschedag AR, Kraume M. Transient rise velocity and mass transfer of a single drop with interfacial instabilities—experimental investigations. *Chem Eng Sci.* 2007;62:2067–2078.
15. Wegener M, Kraume M, Paschedag AR. Terminal and transient drop rise velocity of single toluene droplets in water. *AIChE J.* 2010;56:2–10.
16. Zeng Y, von Klitzing R. Structuring of colloidal suspensions confined between a silica microsphere and an air bubble. *Soft Matter.* 2011;7:5329–5338.
17. Hutter JL, Bechhoefer J. Calibration of atomic-force microscope tips. *Rev Sci Instrum.* 1993;64:1868.
18. Ducker WA, Senden TJ, Pashley, RM. Measurement of forces in liquids using a force microscope. *Langmuir.* 1992;8:1831–1836.
19. Saïen J, Somayeh A. Variations of interfacial tension of the *n*-butyl acetate + water system with sodium dodecyl sulfate from (15 to 22) °C and pH between 6 and 9. *J Chem Eng Data.* 2008;19:525–530.
20. Saïen J, Asadabadi, S. Adsorption and interfacial properties of individual and mixtures of cationic/nonionic surfactants in toluene + water chemical systems. *J Chem Eng Data.* 2010;21:3817–3824.
21. Villers D, Platten JK. Temperature dependence of the interfacial tension between water and long-chain alcohols. *J Phys Chem.* 1988;92:4023–4024.
22. Paul N, Kraume. Influence of non-ionic surfactants on liquid-liquid mass transfer at single droplets. *Czas Tech Mech.* 2012;109:185–194.
23. Miller R, Ferrari M, Ravera F, Liggieri L, Zhlob SA, Fainerman VB, Neumann AW. Messungen der dynamischen Grenzflächenspannung im System wässrige Tensidlösung/organisches Lösungsmittel (in German). *Chem Ing Tech.* 1998;70:89–99.
24. Guo R, Thang X, Guo X. The phase behavior and the structural properties of Triton X-100/*n*-C₈H₁₇OH/PEG1000aq systems. *J Dispersion Sci Technol.* 2001;22:443–451.
25. Zhu DM, Wu X, Schelly ZA. Reverse micelles and water in oil microemulsions of Triton X-100 in mixed solvents of benzene and *n*-hexane. Dynamic light scattering and turbidity studies. *Langmuir.* 1992;8:1538–1540.
26. Daniel RC, Berg JC. Dynamic surface tension of polydisperse surfactant solutions: a pseudo-single component approach. *Langmuir.* 2002;18:5074–5082.
27. Atkins, PW, de Paula J. Physical Chemistry. New York: Oxford University Press, 2006.
28. Menger FM, Rizvi SA. Relationship between surface tension and interfacial coverage. *Langmuir.* 2011;27:13975–13977.
29. Schwurger M, Findenegg G. Lehrbuch der Grenzflächenchemie (in German). Stuttgart: Georg Thieme Verlag, 1996.
30. Attard P, Miklavcic S. Effective spring constant of bubbles and droplets. *Langmuir.* 2001;17:8217–8223.
31. Feng ZG, Michaelides EE. Drag coefficients of viscous spheres at intermediate and high Reynolds numbers. *J Fluid Eng.* 2001;123:841–849.
32. Kraume M. Transportvorgänge in der Verfahrenstechnik: Grundlagen und apparative Umsetzungen “(in German). Berlin: Springer Verlag, 2002.
33. Wegener M, Paul N, Kraume M. Fluid dynamics and mass transfer at single droplets in liquid/liquid systems. *Int J Heat Mass Transfer.* 2014;71:475–495.
34. Martin H. Wärme- und Stoffübertragung in einer Wirbelschicht (in German). *Chem Ing Tech* 1980;52:199–209.
35. Wegener M, Paschedag AR. The effect of soluble anionic surfactants on rise velocity and mass transfer at single droplets in systems with Marangoni instabilities. *Int J Heat Mass Transfer.* 2012;55:1561–1573.
36. Takagi S, Matsumoto Y. Surfactant effects on bubble motion and bubbly flow. *Annu Rev Fluid Mech.* 2011;43:615–636.
37. Kurimoto R, Hayashi K, Tomiyama A. Terminal velocities of clean and fully-contaminated drops in vertical pipes. *Int J Multiphase Flow.* 2012;49:8–23.
38. Clift R, Grace JR, Weber ME. Bubbles, Drops, and Particles. New York: Academic Press, 1998.
39. Lochiel AC, Calderbank P.H. Mass transfer in the continuous phase around axisymmetric bodies of revolution. *Chem Eng Sci.* 1962;19:471–484.

Manuscript received June 10, 2014, and revision received Sept. 23, 2014.